

# Caustics and Intermittency in Turbulent Suspensions of Heavy Particles

J. Bec,<sup>1</sup> L. Biferale,<sup>2</sup> M. Cencini,<sup>3</sup> A. S. Lanotte,<sup>4</sup> and F. Toschi<sup>5,6</sup>

<sup>1</sup>Université de Nice-Sophia Antipolis, CNRS, Observatoire de la Côte d'Azur, Laboratoire Cassiopée, Bd. de l'Observatoire, 06300 Nice, France.

<sup>2</sup>Department of Physics and INFN, Università Tor Vergata, Via della Ricerca Scientifica 1, 00133 Roma, Italy.

<sup>3</sup>INFN-CNR, SMC Dept. of Physics, Università "La Sapienza", P.zzle A. Moro 2, and ISC-CNR, Via dei Taurini 19, 00185 Roma, Italy.

<sup>4</sup>ISAC-CNR, Via Fosso del Cavaliere 100, 00133 Roma, and INFN, Sezione di Lecce, 73100 Lecce Italy.

<sup>5</sup>Department of Physics and Department of Mathematics and Computer Science and J.M. Burgers Centre for Fluid Dynamics, Eindhoven University of Technology, 5600 MB Eindhoven, The Netherlands.

<sup>6</sup>IAC-CNR, Viale del Policlinico 137, 00161 Roma, Italy.

(Dated: September 8, 2021)

The statistics of velocity differences between very heavy inertial particles suspended in an incompressible turbulent flow is found to be extremely intermittent. When particles are separated by distances within the viscous subrange, the competition between quiet regular regions and multi-valued caustics leads to a quasi bi-fractal behavior of the particle velocity structure functions, with high-order moments bringing the statistical signature of caustics. Contrastingly, for particles separated by inertial-range distances, the velocity-difference statistics is characterized in terms of a local Hölder exponent, which is a function of the scale-dependent particle Stokes number only. Results are supported by high-resolution direct numerical simulations. It is argued that these findings might have implications in the early stage of rain droplets formation in warm clouds.

PACS numbers: 47.27.-i, 47.10.-g

Two effects have recently been singled out to explain the speed-up of collisions between small finite-size particles suspended in turbulent flows [1, 2, 3]: *preferential concentration*, that is the development of strong inhomogeneities in their spatial distribution (Fig. 1a) [4, 5, 6], and the formation of *fold caustics* (also called the *sling effect*), which results in large probabilities that close particles have important velocity differences (Fig. 1b) [7, 8, 9]. Improving the collision kernels used in kinetic models for atmospheric physics, astrophysics, and engineering requires quantifying precisely the individual contribution of these two effects and, in particular, to what extent turbulence might affect them, i.e. how they depend on the Taylor-scale Reynolds number  $R_\lambda$  of the flow [10, 11].

In this Letter, to straighten out these questions, we consider suspensions of small, heavy, and dilute particles, which is a setting relevant to the early stage of rain droplets formation in clouds [2]. In these conditions, particles are simply dragged by viscous forces and each individual trajectory  $\mathbf{X}(t)$  solves the equation

$$\tau \ddot{\mathbf{X}} = -\dot{\mathbf{X}} + \mathbf{u}(\mathbf{X}, t), \quad (1)$$

where dots denote time derivatives,  $\mathbf{u}$  the fluid velocity field, solution of the incompressible Navier-Stokes equation, and  $\tau = 2a^2\alpha/(9\nu)$  the Stokes time, depending on particle radius  $a$ , density contrast  $\alpha$  with the fluid, and fluid kinematic viscosity  $\nu$ , see [12] for a recent review. The importance of inertia in the particle dynamics is quantified by the *Stokes number*  $St = \tau/\tau_\eta$ , where  $\tau_\eta$  is the fluid eddy turnover time associated to the Kolmogorov dissipative scale  $\eta$ . The collision rate

between particles is evaluated using the ghost-particle approach [5], which assumes that particles can occupy any point of space independently of the positions of others. This approximation is valid in the asymptotics of very diluted suspensions, and has the advantage of relying on stationary dynamical statistics: the geometrical collision rate is then determined by the value at  $r = 2a$  of the *approaching rate* [7]

$$\kappa(r; St) = - \left\langle \dot{R} \mid R=r \text{ and } \dot{R} \leq 0 \right\rangle p_2(r). \quad (2)$$

Here  $R$  denotes the distance between two particles with Stokes number  $St$ , and  $p_2$  its probability density. The average is performed over time and particle pairs, with the condition to be separated by a distance  $r$  and to approach each other. Clearly the behavior of  $\kappa(r; St)$  prescribes the dependence of the collision rate upon the par-

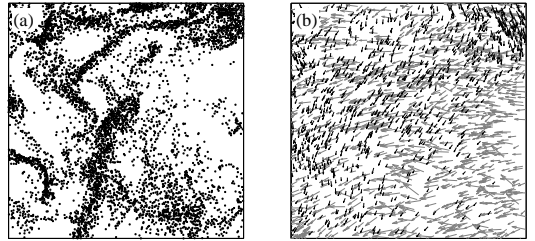


FIG. 1: (a) Snapshot of the position of particles for  $St = 2$  in a slice of size  $5\eta \times 100\eta \times 100\eta$  for  $R_\lambda \approx 400$ . (b) Particle velocity field in the same slice for a larger Stokes,  $St = 20$ , showing the existence of regions where particles have different velocities (highlighted by gray and black arrows).

ticle attributes (size and mass density contrast). Caustics and preferential concentration (Fig. 1) intricately appear in (2) affecting the conditional average of the velocity difference  $\dot{R}$  and the  $r$ -dependence of  $p_2$ , respectively. In particular, as shown in [13],  $p_2(r)$ , which is straightforwardly related to the radial distribution function of [5], behaves as a power law in the dissipative range, namely  $p_2(r) \propto r^{D_2-1}$  for  $r \ll \eta$ , where  $D_2 \in [0:3]$  is the *correlation dimension* of the particle distribution and non-trivially depends on the Stokes number.

We focus here on the velocity contribution by studying the behavior as a function of the separation  $r$  of the longitudinal particle velocity structure functions

$$S_p(r; St) = \left\langle |\dot{R}|^p \mid R=r \right\rangle. \quad (3)$$

The choice of defining structure functions with absolute values is motivated by the definition of the collision kernel (via the approaching rate), since we do not expect important differences between negative and positive velocity fluctuations. One can therefore estimate:  $\kappa(r) \propto r^{D_2-1} S_1(r; St)$  (see [7]). Evaluating  $S_p(r; St)$  for values of  $p$  different from 1, besides providing a more complete characterization of the velocity statistics, allows one to account also for fluctuations of the local approaching rate, which can vary significantly from place to place. In the limit of small inertia, the particle dynamics approaches that of tracers and consequently the velocity difference  $\dot{R}$  is essentially coincident with the fluid longitudinal increment over a separation  $R$ . Conversely, when  $St \rightarrow \infty$ , particles move ballistically in the flow with uncorrelated velocities and the structure functions  $S_p(r; St)$  become independent of  $r$ . For intermediate values of the Stokes number, one expects a non-trivial behavior of  $S_p$  as a function of  $r$  and  $St$ . Data analyzed in this study are from a direct numerical simulation at  $R_\lambda \approx 400$  described in [14, 15].

Figure 2 represents the behavior of the second-order structure function  $S_2(r; St)$ , measured in direct numerical simulations, for two different values of the carrier

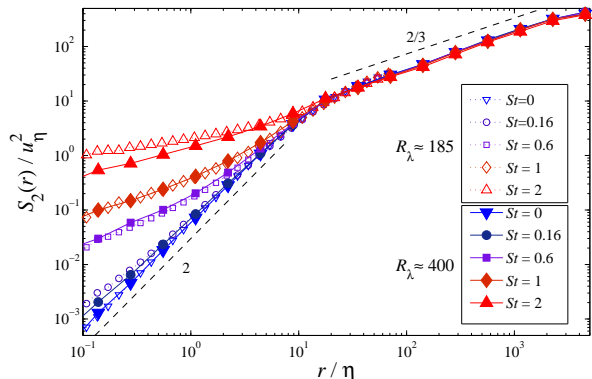


FIG. 2: (color online) Second-order longitudinal velocity structure function for particles with various Stokes numbers and for two Reynolds numbers.

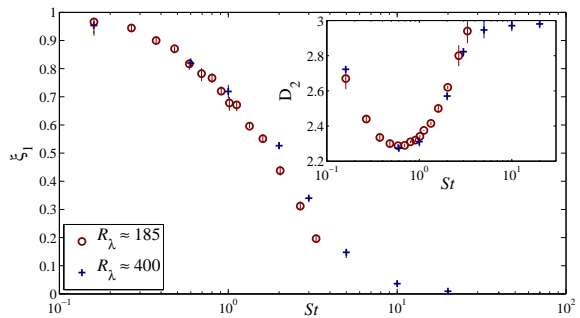


FIG. 3: (color online) Scaling exponent,  $\xi_1$ , vs.  $St$  for two values of  $R_\lambda$ . Inset: correlation dimension  $D_2$  vs.  $St$ .

flow Reynolds number (see [14] for details on the simulations). One distinguishes different regimes, depending whether  $r$  is within the dissipative or inertial range of the turbulent carrier flow. While the dissipative-range behavior directly relates to inter-particle collisions, the inertial-range behavior has important implications on the relative dispersion of particles in turbulent flow [14] in general and for pollution models in particular. In the sequel we investigate these two regimes separately.

In the dissipative range, the structure functions display a power-law behavior  $S_p(r; St) \propto r^{\xi_p}$ . The two asymptotics of weak and strong inertia imply that  $\xi_p \simeq p$  for  $St \ll 1$  and  $\xi_p \rightarrow 0$  for  $St \rightarrow \infty$ . For intermediate values of the Stokes number,  $p \mapsto \xi_p(St)$  is a convex function of the order  $p$  with values in  $[0:p]$ . Figure 3 shows the first-order exponent  $\xi_1$  as a function of the Stokes number. One can clearly observe that for  $St = O(1)$ , the exponent  $\xi_1$  takes non-trivial values spanning the whole interval  $[0:1]$ . The present accuracy of data does not allow for settling either the issue of a possible saturation of the exponent to the limiting values at the two extrema, nor a possible dependence of the exponent upon  $R_\lambda$ . Despite a factor two in  $R_\lambda$ , data differ by less than the errors made in the determination of the exponents or in the value of  $\tau_\eta$  that enters the definition of  $St$ .

At first glance the continuous variation of the exponent  $\xi_1$  from 1 to 0 at increasing  $St$  seems inconsistent with a naive picture of the role of caustics in velocity statistics. Fold caustics are a part of catastrophe theory [16]; they occur when fast particles catch up with slower ones to create regions where several velocities can be found at the same location as in Fig. 1b. If particles conserve their velocity and move ballistically, such caustics will extend over the whole domain (whence the analogy with caustics formed by light rays [8]). The typical velocity difference between two particles becomes in that case independent of their distance, meaning that structure functions tend to a constant as  $r \rightarrow 0$ , and thus  $\xi_p = 0$ . However, there are two clear reasons why this continuous-field picture may fail. First, because of their dissipative dynamics, particles concentrate on dynamical attractors in the position-velocity phase space [7]. Such sets are fractal

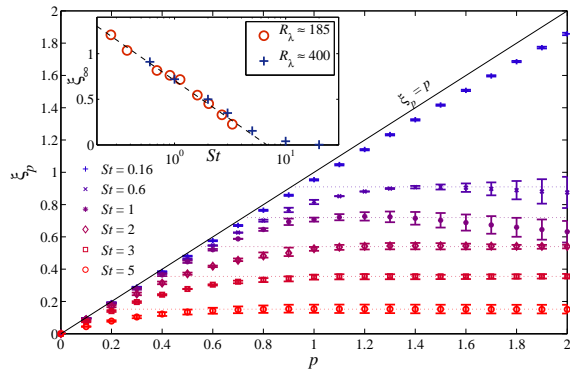


FIG. 4: (color online) Scaling exponents  $\xi_p$  of the particle velocity structure functions  $S_p$  for various  $St$  and  $R_\lambda \approx 400$ . Inset: saturation exponents  $\xi_\infty$  as a function of  $St$  for two values of  $R_\lambda$ . Exponents are obtained by measuring the mean logarithmic derivative of  $S_p(r)$  in  $0.2 \leq (r/\eta) \leq 2$ ; errors correspond to the largest deviations observed in the fitting range.

and correlated with the fluid and lead to the formation of caustics of various strength with non-trivial probabilities. Second, as the particle velocity relaxes to the fluid velocity, the spatio-temporal extent of such caustics may also have complex statistical properties.

To better quantify the contribution from caustics, we extend our investigation to the particle velocity scaling exponents  $\xi_p$ 's with orders  $p$  other than 1, shown in Fig. 4 for various values of the Stokes number. At small orders, the exponents are almost tangent to the line  $\xi_p = p$  while, at large orders, they approach or saturate to an asymptotic value  $\xi_\infty$ , monotonically decreasing with  $St$  as shown in the inset. Numerical data suggests that  $\xi_\infty \propto \ln(1/St)$  for  $St \lesssim 7$  and that  $\xi_\infty \simeq 0$  for  $St \gtrsim 7$ . The current numerical accuracy does not enable distinguishing between a sharp and smooth transition at  $St \simeq 7$ . However, we notice that the estimated value of such a critical Stokes number is very close to that for which  $D_2 \approx 3$  (see inset of Fig. 3). As discussed in [10] a saturation of  $D_2$  to the space dimension is indeed expected for  $St$  values at which caustics become dominating. In this respect, we also notice that the saturation exponent  $\xi_\infty$  can be interpreted as the co-dimension of large fold caustics associated to order-unity velocity jumps. Indeed, such caustics contribute to the structure function  $S_p(r; St)$  a term of the form  $V_p P(r)$  where  $V_p$  is the  $p$ -th order moment of the velocity difference inside the caustics and  $P(r)$  is the probability of having such a caustic present in a box of size  $r$ . The saturation of the scaling exponents suggests that  $P(r) \propto r^{-\xi_\infty}$ , so that  $D^{(c)} \equiv 3 - \xi_\infty$  is the (statistical) Hausdorff dimension of the set of caustics. At smaller orders, the statistics is dominated by other events for which one can figure out two conceivable scenarios. A first possibility is that caustics distribution spans all possible sizes with non-trivial co-dimensions, i.e. is a multi-fractal. In this case they affect all orders and give rise to multiscaling and to a non-trivial behavior of the exponents  $\xi_p$  before the saturation [17]. The alternative possibility is that

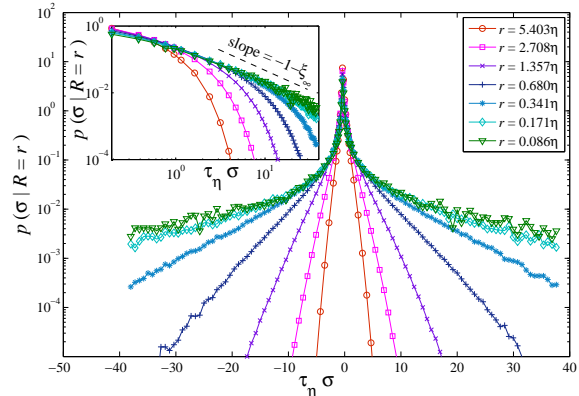


FIG. 5: (color online) Probability density of the (rescaled) longitudinal velocity difference  $\sigma = \dot{R}/R$  for various values of  $r$  and for  $St = 3.3$  and  $R_\lambda \approx 185$ . Inset: same for the right tail in log-log coordinates.

the caustics are randomly distributed with a typical size and dominate the velocity statistics at large moments only, while small orders are controlled by the smooth regions of the particle velocity. In that case the structure function would display a bi-fractal behavior similar to that present in random solutions to the Burgers equation (see, e.g., [18]), namely  $\xi_p = p$  for  $p \leq \xi_\infty$  and  $\xi_p = \xi_\infty$  for  $p \geq \xi_\infty$ . Current numerical results do not permit to distinguish between these two possibilities. As seen from Fig. 4, the measured exponents show some deviations from the bi-fractal behavior. However as already observed in other settings [19], this apparent multiscaling could be an artifact due to the presence of sub-leading terms or logarithmic corrections.

To further disentangle the question of the contribution of caustics to velocity scaling, we investigate the statistical properties of  $\sigma = \dot{R}/R$ , which can be interpreted as a longitudinal velocity gradient of an effective particle velocity field. This quantity is at the center of much work devoted to the relative motion of a pair of particles in time-uncorrelated flows [8, 20, 21, 22]. There, the dynamics of  $\sigma$  becomes independent of  $R$  at very small scales, a far from obvious feature for particles transported by real flows, where time correlations and structures play important roles. Further, results in random flows suggest that the conditional probability density  $p(\sigma | R=r)$  is independent of  $\sigma$  at small scales and has power-law tails. As seen from Fig. 5, numerical measurements in turbulent flows suggest features similar to those of structure-less random flows. The core of the distributions associated to different scales  $r$  collapse for  $|\sigma| \lesssim \sigma^*(r)$  on a distribution with a fat, almost algebraic behavior. Interestingly, the associated power-law exponent is close to  $-(1 + \xi_\infty)$ , suggesting that  $\langle \sigma^p \rangle$  diverges for  $p > \xi_\infty$ , a behavior favoring the bi-fractal scenario. Indeed  $S_p(r; St) = r^p \langle \sigma^p | R=r \rangle \simeq r^p \langle \sigma^p \rangle$  for  $r \rightarrow 0$  and  $p$  such that  $\langle \sigma^p \rangle < \infty$ . However, for  $|\sigma| \gtrsim \sigma^*(r)$ , the distributions display stretched-exponential tails, whose contribution to the structure function is for the moment unsettled. They are connected to the caustics size prob-

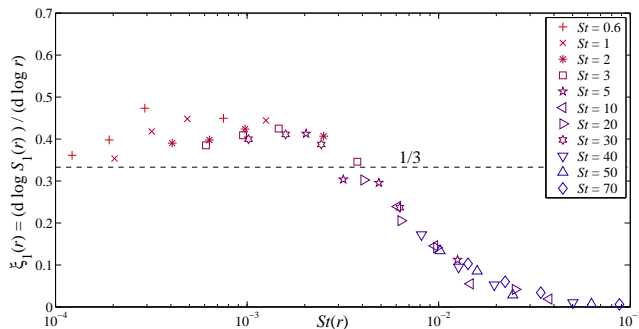


FIG. 6: (color online) First-order local exponent  $\xi_1(r)$  as a function of the local Stokes number  $St(r)$  for  $R_\lambda \approx 400$ . The horizontal dashed line represents tracers K41 expectation.

ability distribution and could lead to multiscaling. A related open question is the non-trivial entanglement between clusters and large velocity differences, as already stressed in random flows [23]. This latter feature might imply an intricate dependence on  $r$  of velocity difference statistics, that might lead to multiscaling. Settling numerically the issue of bi- versus multiscaling would require to explore systems where statistics can be handled in a more systematic way, as for instance in random correlated flows or real flows at smaller Reynolds numbers.

We finally turn to the behavior of the velocity structure function for separations within the inertial range of turbulence, i.e. for  $\eta \ll r \ll L$ . As seen from Fig. 2, particle velocity structure functions recover the fluid ones when  $r$  becomes very large. Indeed as  $r$  increases the associated eddy turnover time grows as  $r^{2/3}$  (where we used the Kolmogorov 1941 scaling) so that the effective strength of inertia reduces. Similarly to random self-similar carrier flows [22], this effect can be put on a quantitative ground in terms of a scale-dependent Stokes number  $St(r) = \varepsilon^{1/3} \tau / r^{2/3}$  defined as the ratio between the particle response time and the turnover time associated to the scale  $r$ , where  $\varepsilon$  denotes the mean dissipation rate of kinetic energy. We check whether the local scaling exponent  $\xi_p(r; \tau) \equiv (d \ln S_p(r; St)) / (d \ln r)$  does depend on  $St(r)$  only, as observed in random self-similar flows [22]. Figure 6 shows a good collapse of the values of  $\xi_1(r, \tau)$  associated to various  $\tau$  and of  $r$ , once represented as a function of  $St(r)$ . Moreover, the curve  $\xi_1(St(r))$  has a shape qualitatively very similar to that of  $\xi_1(St)$  observed in the dissipative range and shown in Fig. 3, this fact is relevant to heavy particle dispersion in turbulent flows [14]. Let us stress that data corresponding to small  $St(r)$  in Fig. 6 show deviations from the K41 scaling that are similar to those expected for tracers-like statistics.

To conclude we briefly discuss the applicability of the present results to atmospheric physics. The main shortcoming of the proposed approach is that the gravity force is neglected. As observed in [24] for dynamics of water droplets in warm clouds, gravitational settling is found to dominate the statistics of velocity differences between

particles. However, this effect acts mainly between particles of different sizes that fall at different speeds. Present results should apply to earlier stage of rain formation during which the droplets are almost mono-disperse and might play an important role in explaining the observed fast spectral broadening observed in clouds.

This study benefited from fruitful discussions with L. Collins, G. Falkovich, B. Mehlig, L.-P. Wang, and M. Wilkinson. JB and AL acknowledge support from NSF under grant No. PHY05-51164. Part of this work was supported by ANR under grant No. BLAN07-1-192604. Simulations were performed at CASPUR and CINECA (Italy), and in the framework of the DEISA Extreme Computing Initiative supported by the DEISA Consortium (co-funded by the EU, FP6 project 508830).

- 
- [1] S. Sundaram and L.R. Collins, *J. Fluid Mech.* **335**, 75 (1997).
  - [2] G. Falkovich, A. Fouxon, and M. Stepanov, *Nature* **419**, 151 (2002).
  - [3] R.A. Shaw, *Ann. Rev. Fluid Mech.* **35**, 183 (2003).
  - [4] L.-P. Wang, A.S. Wexler, and Y. Zhou, *Phys. Fluids* **10**, 1206 (1998).
  - [5] W.C. Reade and L.R. Collins, *Phys. Fluids* **12**, 2530 (2000).
  - [6] S. Goto and J.C. Vassilicos, *Phys. Rev. Lett.* **100**, 054503 (2008).
  - [7] J. Bec *et al.*, *Phys. Fluids* **17**, 073301 (2005).
  - [8] M. Wilkinson and B. Mehlig, *Europhys. Lett* **71**, 186 (2005); M. Wilkinson, B. Mehlig, and V. Bezuglyy, *Phys. Rev. Lett.* **97**, 048501 (2006).
  - [9] G. Falkovich and A. Pumir, *J. Atmos. Sci.* **64**, 4497 (2007).
  - [10] S. Derevyanko, G. Falkovich, and S. Turitsyn, *New J. Phys.* **10**, 075019 (2008).
  - [11] Y. Xue, L.-P. Wang, and W. Grabowski, *J. Atmos. Sci.* **65**, 331 (2008).
  - [12] F. Toschi and E. Bodenschatz, *Ann. Rev. Fluid Mech.* **375**, 41 (2009).
  - [13] J. Bec *et al.*, *Phys. Rev. Lett.* **98**, 084502 (2007).
  - [14] J. Bec *et al.*, “Turbulent pair dispersion of inertial particles”, preprint arXiv:0904.2314.
  - [15] Raw data of particle trajectories are freely available from the iCFDdatabase (<http://cfd.cineca.it>).
  - [16] V.I. Arnold, S.F. Shandarin, and Ya.B. Zel’dovich, *Geophys. Astrophys. Fluid Dyn.* **20**, 111 (1982).
  - [17] A. Celani *et al.*, *Phys. Rev. Lett.* **84**, 2385 (2000).
  - [18] J. Bec and K. Khanin, *Phys. Rep.* **447**, 1 (2007).
  - [19] L. Biferale *et al.*, *New J. Phys.* **6**, 37 (2004); D. Mitra *et al.*, *Phys. Rev. Lett.* **94**, 194501 (2005).
  - [20] L.I. Piterbarg, *SIAM J. Appl. Math.* **62**, 777 (2002).
  - [21] S. Derevyanko *et al.*, *J. Turbulence* **8**, 1 (2007).
  - [22] J. Bec *et al.*, *Physica D* **237**, 2037 (2008).
  - [23] P. Olla, *Phys. Rev. E* **77**, 065301 (2008).
  - [24] O. Ayala, B. Rosa, and L.-P. Wang, *New J. Phys.* **10**, 075016 (2008).